Axial Mixing in a Reciprocating Plate Column with Very Small Density Gradients

Malcolm H. I. Baird and N. V. Rama Rao
Dept. of Chemical Engineering, McMaster University, Hamilton, Ontario, Canada L8S 4L7

Axial dispersion coefficients have been measured in single-phase flow conditions in a 5.08-cm-dia. reciprocating plate extraction column. The measurements were done under steady-state conditions by analyzing temperature profiles (for hot and cold water mixing) and concentration profiles (for mixing of water and salt solutions). The results confirm previous published data of Holmes et al. (1991) in showing that axial dispersion is increased strongly in the unstable situation, where liquid density increases with height. The earlier work is extended to the condition where buoyant energy dissipation is exceeded by mechanical energy dissipation by four orders of magnitude. Even in this case, axial mixing is increased significantly by density gradient-induced instability. Results have been correlated by a simple equation based on a mixing length model.

Introduction

Axial mixing must be taken into account in designing countercurrent contactors, when the superficial-phase velocities are low, as in the case of solvent extraction. The review by Pratt and Baird (1983) summarizes the methods of calculating the axial mixing effects on the effective height of a transfer unit. The principal factors determining the value of the axial dispersion coefficient under given conditions include the flow rates of each phase, the design of the column internals, and the level of agitation employed. Another important factor is "hydraulic nonuniformity," which was first discussed in detail by Rosen and Krylov (1974) and is known to increase strongly with the diameter of the column employed.

Holmes et al. (1991) have examined the effect of an adverse (unstable) axial density gradient on axial dispersion coefficients in a 7.62-cm-dia. reciprocating plate column of the type developed originally by Karr (1959). The experiments were carried out under steady-state conditions, with a dense calcium chloride solution injected at the top of the column, while pure water was fed to the bottom of the column. The downward back-mixing of the calcium chloride was measured by taking samples at different points in the column.

It was found (Holmes et al., 1991) that all data could be correlated empirically in terms of the specific energy dissipation rates, expressed in W/kg (SI units) or $cm^2 \cdot s^{-3}$ units, which are equivalent to 10^{-4} times the SI unit dissipation rate.

$$E = 9.52\epsilon_b^{0.535}\epsilon_t^{-0.186} \tag{1}$$

The units in Eq. 1 are in the centimeter and second system, so that E can be expressed as cm^2/s. The buoyant dissipation term ϵ_b is calculated from the local difference between the density of the solution and that of pure water.

$$\epsilon_b = \frac{gU\Delta\rho}{\rho} \tag{2}$$

The specific energy dissipation rate due to mechanical agitation is calculated (Hafez and Baird, 1978) from the agitation stroke and frequency as follows.

$$\epsilon_m = \frac{2\pi^2}{3}\left(\frac{1-S^2}{C_0^2 S^2}\right)\frac{(Af)^3}{h} \tag{3}$$

The total specific energy dissipation is thus

$$\epsilon_t = \epsilon_b + \epsilon_m \tag{4}$$

Equation 1 was found to fit the extensive data of Holmes et al. (1991) with a standard deviation of 17.9%. The equation indicates that axial mixing is *reduced* by agitation and the effect was attributed to a reduction in the mixing length due to a reduction in the turbulence scale, as agitation was increased.

Two limiting cases

In the absence of any plate agitation, $\epsilon_m = 0$ and Eq. 1 becomes simply

$$E_o = 9.52\epsilon_b^{0.349} \tag{5}$$

That relationship was confirmed by Holmes et al. (1991), with E_o in the range 12 to 58 cm^2/s depending on the value of ϵ_b.

The second limiting case is the one in which buoyancy effects are negligible. That case was not examined by Holmes et al. who considered only data for which the density difference exceeded 0.01 g/mL. In the limiting case of $\Delta\rho = 0$ and hence $\epsilon_b = 0$, it would appear from Eq. 1 that $E = 0$. However, typical observed values of E in the absence of buoyancy effects are in the order 1 to 3 cm^2/s, as noted previously by Kim and Baird (1976) and by Hafez et al. (1979).

It is the purpose of this study to provide data on the effects of extremely low unstable density differences and to develop an amended correlation that is consistent both with the work of Holmes et al. (1991) and with earlier data on axial mixing in the absence of any buoyancy effects. This is achieved by using hot and cold water, which have an extremely small, but well-documented, density variation; some data have also been obtained with dilute sodium chloride solutions as tracers.

Experimental Studies

Systems investigated

Figure 1 shows the density of water as a function of temperature (Perry et al., 1984). In this work, the temperature range for hot/cold water was approximately 20°C to 70°C providing a maximum variation of density of 0.02 g/mL. It is important to note that density is not a linear function of temperature over this range; special calculation techniques are required for the buoyant energy dissipation, as will be discussed later. In the case of sodium chloride/water solutions (Figure 1), the density is linearly proportional to salt concentration. The maximum variation of density was 0.11 g/mL.

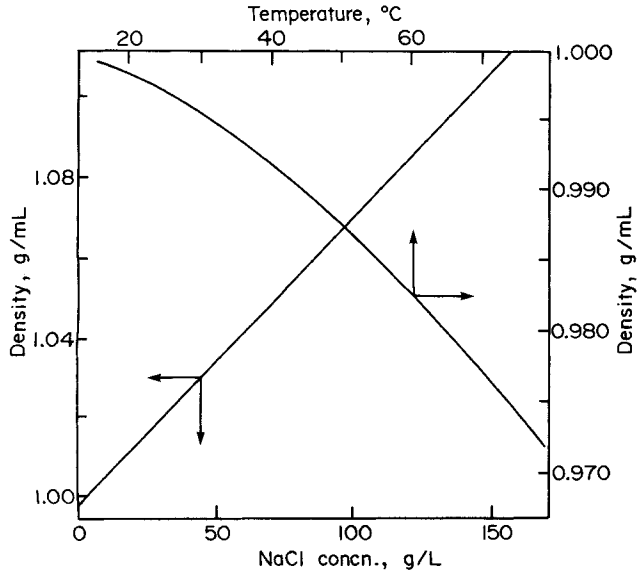

Figure 1. Density/temperature for water and density/composition plot (20°C) for aqueous sodium chloride solutions.

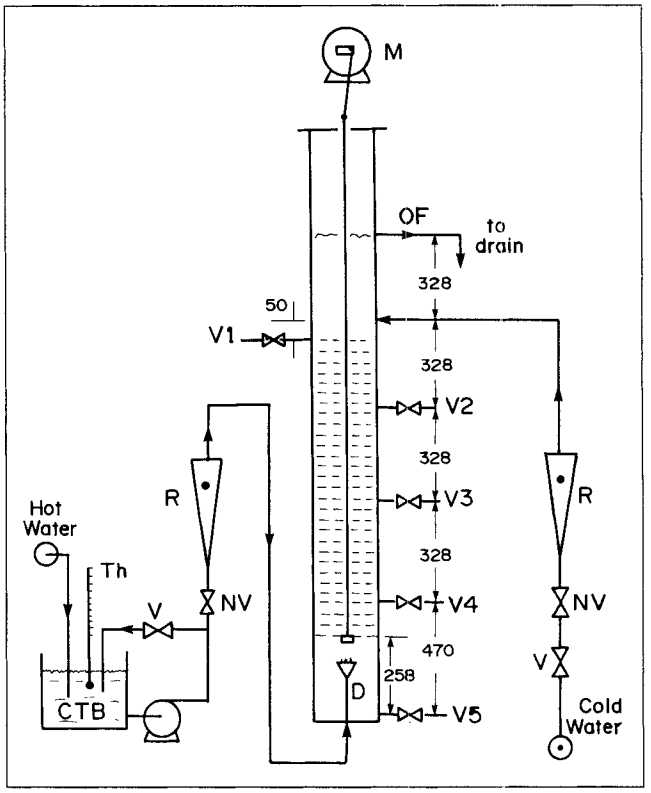

Figure 2. Reciprocating plate column and ancillaries for hot/cold water mixing tests.

CTB = constant temperature bath
D = distributor
M = driver motor
Th = thermometer
Dimensions are in mm.
NV = needle valve
R = rotameter
OF = overflow
V1-V5 = sample points
V = valve

Equipment

Figure 2 shows the 5.08-cm-ID reciprocating plate column and ancillaries. The column was of flanged glass sections with total height 2.3 m. It contained a central drive shaft supporting a stack (height 1.146 m) of stainless steel plates mounted at intervals h of either 2.7 cm or 5.2 cm. Each plate was provided with 12.7-mm holes and had a fractional open area of 0.57. The plate stack was driven from above by a variable-speed electric motor coupled by a yoke; the stroke A was set at either 1.8 cm or 2.8 cm for hot/cold water and at 2.9 cm for salt solutions. The frequency could be set between 0 and 5 Hz.

The mixing was carried out with a denser liquid near the top of the stack, while the lighter liquid was injected beneath the stack and rose up through it at a superficial velocity U. Figure 2 shows the arrangement with hot water entering the bottom and mixing at the top of the column with an excess of cold water, before leaving via an overflow. The analogous arrangement with sodium chloride solution at the top and pure water at the bottom is not shown here, but was similar to that described by Holmes et al. (1991) for calcium chloride.

In the case of hot/cold water, it was important to avoid heat

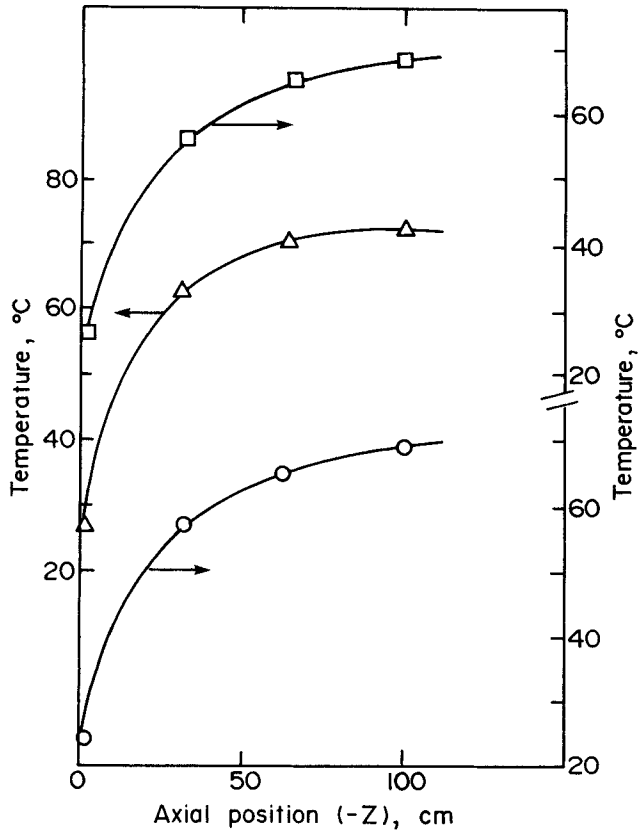

Figure 3. Typical temperature profiles.

$U = 0.204$cm/s, $h = 5.2$ cm

Af (cm/s):	0	2.91	11.5
Data point symbol:	o	Δ	□

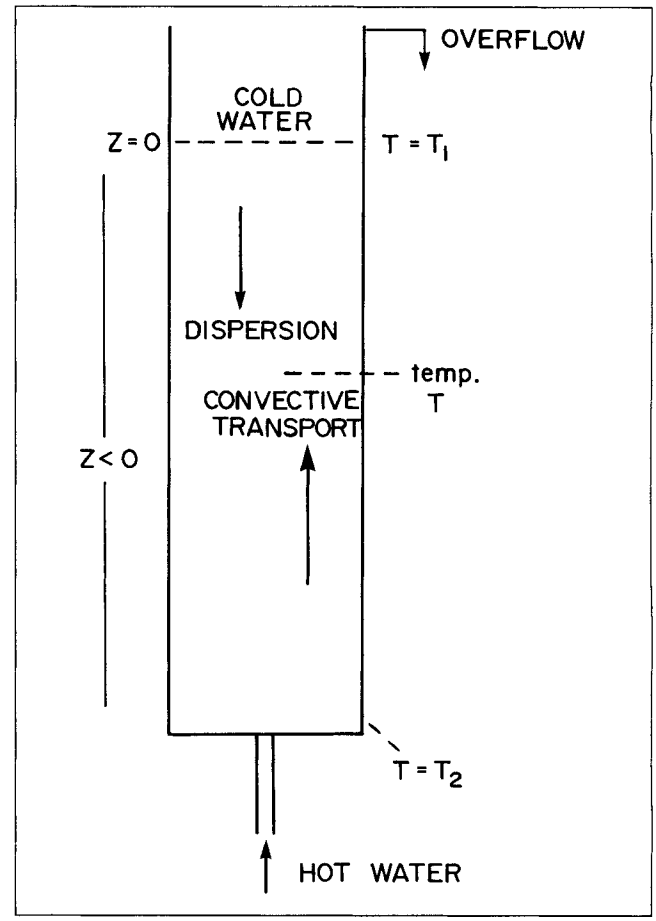

Figure 4. Basis of Eq. 7b.

losses from the column, which was therefore insulated. The hot water was fed from a tank at about 80°C, but entered the column at about 75°C. Superficial velocities of between 0.15 and 0.3 cm/s were employed. Cold water entered near the top of the plate stack slightly below ambient temperature. It was fed at a flow at least five times greater than that of the hot water, so that the temperature of the mixed overflow at OF (Figure 2) was between 20°C and 25°C. The temperatures were measured for liquid sampled at five different points VI through V5 as shown in Figure 2. Hence, the temperature profile along the plate stack (points V1 to V4) could be plotted. The temperature at V5 provided a boundary condition for the water at the base of the column.

Data Processing

Figure 3 shows a typical set of temperature profiles in the absence of agitation, at three different agitation levels. It is apparent that the temperature gradient is the greatest at the top of the stack where the cold water flow is maintained. To convert this data to values of the axial dispersion coefficient, a mixing process is considered between the cold liquid at the top of the column (temperature T_1) and the hot liquid entering at the base of the column, sampled at point V5 on Figure 2 (temperature T_2). The conditions are shown in Figure 4. The mass fraction of cold liquid at any axial position beneath the top of the column ($z < 0$) can be related to the mixture temperature assuming adiabatic conditions and constant specific heats:

$$x = \frac{T - T_2}{T_1 - T_2} \tag{6}$$

The net axial transport of cold liquid is zero; upward convection is balanced by downward dispersion under the influence of the density difference. The steady-state conservation equation for a tracer solute is:

$$0 = Uc - E\frac{dc}{dz} \tag{7a}$$

where U is the superficial velocity of the liquid entering the column. This form applies for the mixing of a soluble salt, for example, sodium chloride in this work or calcium chloride in the work of Holmes et al. (1991). In the case of the cold water mixing back into the hot water, the conservation equation can be written analogously, assuming adiabatic conditions.

$$0 = Ux - E\frac{dx}{dz} \tag{7b}$$

It should be noted that the thermal diffusivity of water

(1.4×10^{-3} cm^2/s) is several orders of magnitude smaller than the values of E being measured. It is assumed here that the superficial velocity at any point in the plate stack is unaffected by the density changes; this assumption is reasonable in this work involving very small density changes in the order of 1%. In the previous work (Holmes et al., 1991), a small correction had been needed because density changes up to 20% occurred. A rearrangement of Eq. 7a gives:

$$E = Uc/\frac{dc}{dz} \tag{8a}$$

This may also be written in terms of temperature by substituting for x from Eq. 6 into Eq. 7b and rearranging:

$$E = U(T - T_2)/\frac{dT}{dz} \tag{8b}$$

The accuracy of the value of E is limited mainly by the accuracy with which the local temperature gradient can be estimated from the measured profiles as in Figure 3.

Results

A typical set of values of E obtained from the temperature profiles with hot/cold water is given in Figure 5. The values in the absence of agitation show a general downward trend toward the right of the plot, which corresponds to the lower sections of the column. In these sections, the temperature profiles become flatter (Figure 3), and so the density gradients decrease, leading to reduced axial mixing. However, it is also seen that at the top of the column ($z = 0$), the value of E appears to be slightly reduced in some cases. Here, the temperature gradient is very high and difficult to estimate accurately. Moreover, the top sample point is above the top of the plate stack. For these reasons, the apparent values of E at $z = 0$ were not included in the data evaluation. It is important to recall that it is the density gradient which affects E, not the temperature gradient. For the hot/cold water system,

$$\frac{d\rho}{dz} = \frac{dT}{dz}\cdot\frac{d\rho}{dT} \tag{9}$$

The application of very low levels of mechanical agitation (triangles in Figure 5) leads to a considerable reduction in E, as much as 50% below the value in the absence of agitation. The variation of E with axial position shows the same trends. Intense mechanical agitation (squares in Figure 5) results in values of E that are intermediate between the values with zero and low agitation; clearly, E passes through a minimum value as agitation is increased from zero. This effect is discussed below after model development. Another interesting point is that under intense agitation, the axial variation of E is reduced considerably; the effects of the varying local density gradient on E are smaller under well-agitated conditions.

Mixing length model in the absence of mechanical agitation

Holmes et al. (1991) found that their results were consistent

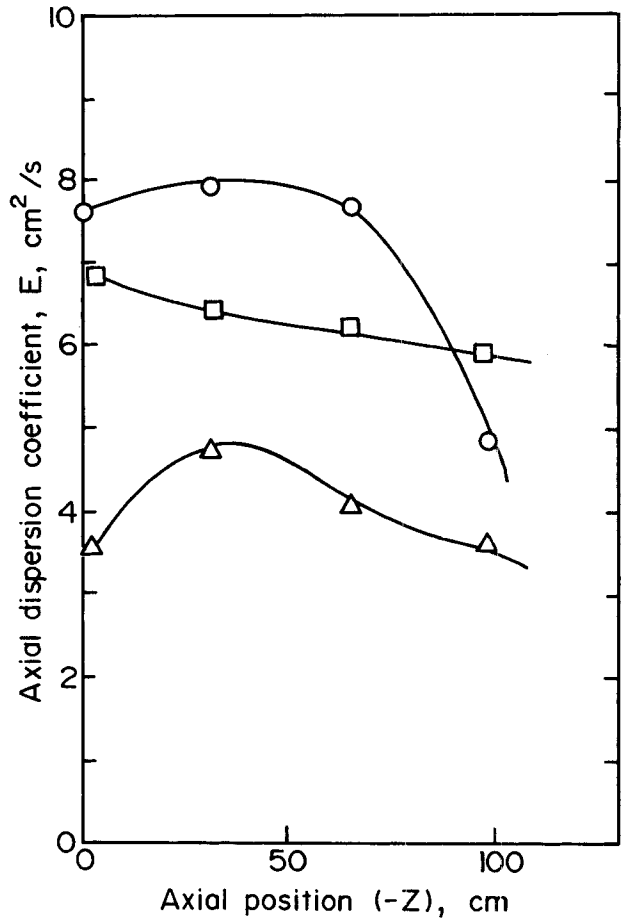

Figure 5. Typical measured values of E for hot/cold water system.

$U = 0.204$ cm/s, $h = 5.2$ cm. For symbols, see Figure 3.

with a simple model based on a characteristic mixing length ℓ similar to that used by Baird and Rice (1975).

$$E = \ell^2\left(\frac{g}{\rho}\cdot\frac{d\rho}{dz}\right)^{1/2} \tag{10}$$

For the special case of steady-state back-mixing with a system in which density was a linear function of concentration, it was shown that in the absence of agitation Eq. 10 led to the expression:

$$E = E_o = \ell^{4/3}(Ug\Delta\rho/\rho)^{1/3} \tag{11}$$

This type of equation was proposed originally by Baird and Rice (1975) for gas-liquid and liquid-liquid flow and has been found effective; ℓ is about 0.45 times the column diameter in the absence of fixed intervals. The exponent 0.349 in Eq. 5 is close to the value 1/3 predicted above. The value of ℓ was thus 5.3 cm or about 70% of the column diameter (Holmes et al., 1991).

In the case of the hot/cold water system, Eq. 10 does not lead to Eq. 11 because the density of water is not a linear function of temperature. The relationship for nonlinear density dependence can be derived from Eqs. 8b, 9 and 10 by elimi-

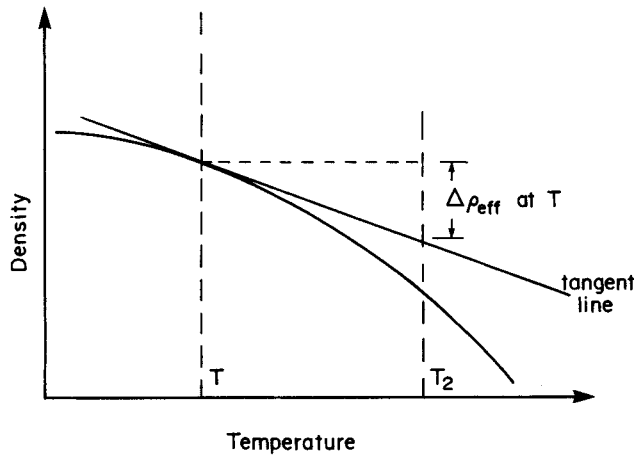

Figure 6. Construction showing effective density difference (Eq. 14).

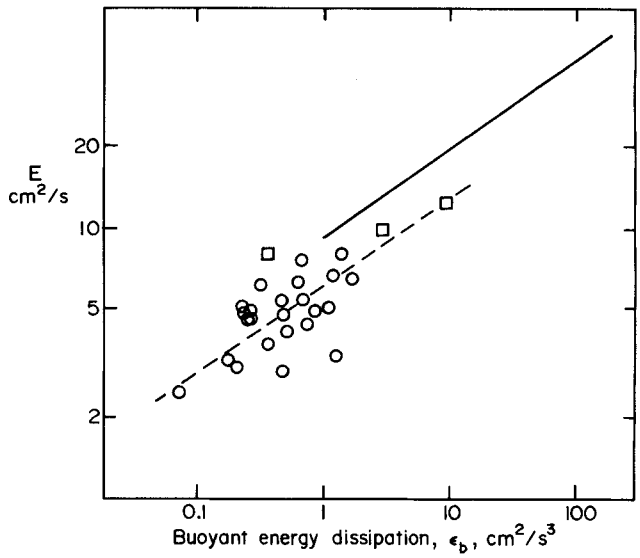

Figure 7. Effect of buoyant energy dissipation rate on axial dispersion coefficient in absence of agitation.

Lines denote Eq. 11.
——— Holmes et al. (1991) with ℓ = 5.3 cm, column diameter 7.62 cm
- - - - This work with ℓ = 4.0 cm, column diameter 5.08 cm
O hot/cold water □ salt solution

nating $(d\rho/dz)$ and (dT/dz) to give:

$$E=\ell^{4/3}\left[Ug(T-T_2)\frac{d\rho}{dT}/\rho\right]^{1/3} \tag{12}$$

In this equation, $d\rho/dT$ is the *local* value at temperature T within the column. Thus, the effective local energy dissipation rate for the hot/cold water system is:

$$\epsilon_b=Ug(T-T_2)\frac{d\rho}{dT}/\rho \tag{13}$$

This is analogous to Eq. 2 with

$$\Delta\rho=\Delta\rho_{\text{eff.}}=(T-T_2)\frac{d\rho}{dT} \tag{14}$$

The relationship between $\Delta\rho_{\text{eff}}$ and the density/temperature curve is shown by the construction on Figure 6.

Figure 7 shows the measured values of E in the absence of agitation, plotted against ϵ_b which is calculated from Eq. 13 for hot/cold water and from Eq. 11 in the case of salt solutions. Also shown is Eq. 11 based on the results of Holmes et al. (1991). In the latter case, the lowest value of ϵ_b was 2 cm^2/s^3 (or 2×10^{-4} W/kg), whereas in the present work ϵ_b was as low as 0.1 cm^2/s^3 (10^{-5} W/kg). The scatter of data points reflects the difficulty of getting reproducible behavior at such low energy dissipation levels. However, the data do conform approximately to the 1/3 power dependence on ϵ_b as expected from Eq. 11. The mixing length ℓ in this work was approximately 4 cm as compared to 5.3 cm for the data of Holmes et al. (1991). It is believed that this difference is due mainly to the differences of internal column diameter; 5.08 cm in this work and 7.62 cm for Holmes et al. (1991). The mixing lengths are 70% and 79% of the column diameter, respectively.

Mixing length model with mechanical agitation

When mechanical agitation is applied, the axial dispersion coefficient is expressed in terms of the mixing length and the total specific energy dissipation rate:

$$E=\ell^{4/3}\epsilon_t^{1/3} \tag{15}$$

where ϵ_t is given by Eq. 4. When Eq. 15 is combined with Eq. 1 based on the data of Holmes et al. (1991), the following expression for ℓ is obtained.

$$\ell=5.4\epsilon_b^{0.401}/\epsilon_t^{0.389} \tag{16a}$$

where the unit of length is centimeter. This equation can be slightly adjusted with little loss of accuracy to give:

$$\ell=5.3(\epsilon_b/\epsilon_t)^{0.40} \tag{16b}$$

This shows that the mixing length in the absence of agitation is 5.3 cm and that it decreases progressively as the level of agitation is increased, that is, as buoyant energy dissipation forms a smaller fraction of total energy dissipation. Holmes et al. (1991) explained this as a reduction in eddy size due to the action of the reciprocating plates.

As discussed earlier, the above equation does not realistically describe the limiting case of $\epsilon_b = 0$. In this case, the mixing length will clearly not go to zero, although a very small value would be expected. It is proposed here that the mixing length varies between a low limit ℓ_m (determined by mechanical energy dissipation) and an upper limit ℓ_b which is in the order of 70% to 80% of the column diameter. It is further proposed that the contributions of mechanical and buoyant energy to the mixing length are of the form:

$$\ell=\ell_m+(\ell_b-\ell_m)(\epsilon_b/\epsilon_t)^n \tag{17}$$

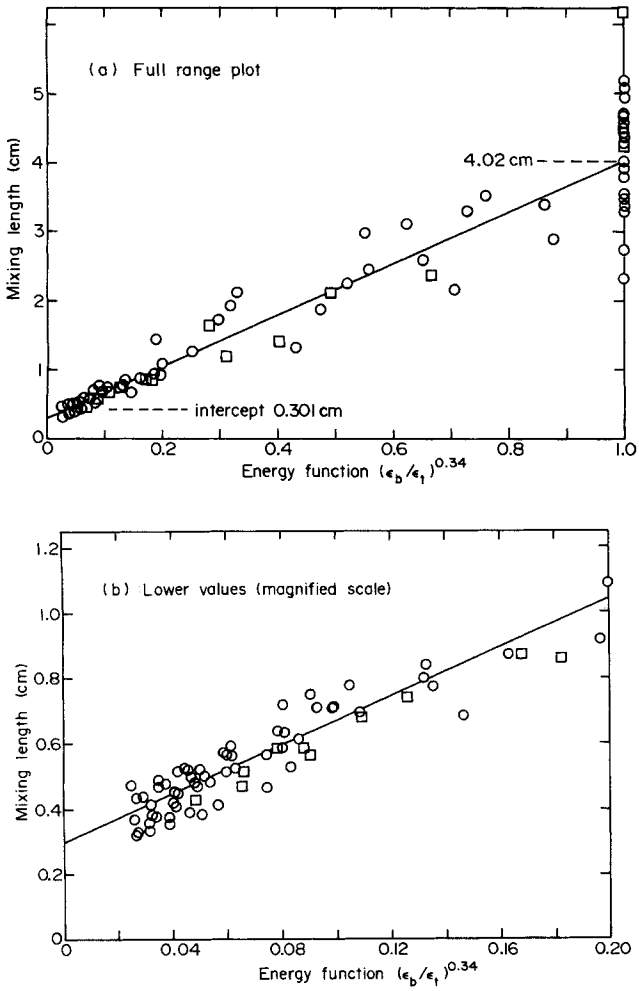

Figure 8. Effect of energy ratio on mixing length.

Lines represent Eq. 17 with ℓ_m = 0.301 cm, ℓ_b = 4.02 cm, and n = 0.34.
O hot/cold water □ salt solution

If Eq. 16b is applied to the case where $\ell_m \ll \ell_b$, it would appear that the exponent is 0.40 according to the data of Holmes et al. (1991).

The values of ℓ_m, ℓ_b and n have been obtained by analysis of 120 data points from this work, both for hot/cold water and salt solutions. For an assumed value of n, the values of ℓ_m and ℓ_b were determined by linear regression and the error sum of squares was also calculated. The procedure was repeated with different values of the exponent n until the error sum of squares was minimized. The result of this analysis gave n = 0.34, ℓ_m = 0.301 cm, and ℓ_b = 4.02 cm. The fitted function and the data are plotted in Figures 8a and 8b, with the latter being an enlarged view of the congested part of Figure 8a. As in the case of Figure 7, the data points are somewhat scattered, but the linear trend is clear. There is no significant difference between the results for hot/cold water and salt solutions. These experiments have indicated that ℓ_m is an order of magnitude smaller than ℓ_b.

Correlation for axial dispersion coefficient

When Eqs. 15 and 17 are combined with n = 0.34, the following expression for E is obtained:

$$E=[\ell_m+(\ell_b-\ell_m)(\epsilon_b/\epsilon_t)^{0.34}]^{4/3}\epsilon_t^{1/3} \tag{18}$$

In the limiting case of $\epsilon_m = 0$ and $\epsilon_t = \epsilon_b$, this leads to Eq. 11 which has been substantiated by Holmes et al. (1991) and in Figure 7 of this work.

In the second limiting case of $\epsilon_b = 0$ and $\epsilon_t = \epsilon_m$,

$$E=E_m=\ell_m^{4/3}\epsilon_m^{1/3} \tag{19}$$

If ϵ_m is taken from Eq. 3 with the typical values of S = 0.57 and C_o = 0.6, then in the absence of buoyancy effects

$$E_m=3.36\ell_m^{4/3}Afh^{-1/3} \tag{20}$$

Equation 20 is consistent dimensionally. If we further take the present value of the mechanical mixing length as 0.301 cm, we obtain

$$E_m=0.678Afh^{-1/3} \tag{21}$$

with length units in centimeter. Thus, for the case h = 2.7 cm, $E = 0.49(Af)$. This is quite close to the results of Baird and Rama Rao (1988) who found that in a 5.08-cm column with h = 2.7 cm, $E \simeq 0.55(Af)$ under single-phase flow conditions without any density gradient.

The data of Holmes et al. (1991) have been compared with Eq. 18, using their value of ℓ_b = 5.3 cm, and the value of ℓ_m = 0.301 cm from this work. The plot of data was noticeably nonlinear, and there was no intercept value of ℓ_m. However, at high agitation levels the calcium chloride concentration profiles were very steep (Holmes et al., 1991) and the slopes were hard to measure accurately. Moreover, only 16 data points occur in the region where $(\epsilon_b/\epsilon_t)^{0.34} < 0.2$, whereas in this work (Figure 8b) that region is more thoroughly explored with 72 data points.

A direct comparison between some of the present data for E and the correlation (Eq. 18) is made in Figure 9. In making such a comparison it is not possible to find many data points at a fixed value of ϵ_b, since this variable could not be set independently. Therefore, two sets of data collected within certain ranges of ϵ_b were compared with curves based on Eq. 18 for the midpoint values of ϵ_b in each case. Also shown in Figure 9 is the limiting case of $\epsilon_b = 0$ as represented by Eq. 21.

Enhancement of axial dispersion by buoyancy effects

The sensitivity of axial dispersion coefficients to small buoyancy effects can be expressed as a ratio E/E_m where E_m is the value (Eq. 19) that would be expected in the absence of buoyancy. The enhancement due to buoyancy is found by dividing Eq. 18 by Eq. 19:

$$E/E_m=\{1+[(\ell_b/\ell_m)-1](\epsilon_b/\epsilon_t)^{0.34}\}^{4/3}(\epsilon_t/\epsilon_m)^{1/3} \tag{22a}$$

With the further assumption that the buoyant energy dissipation is small, it can be stated that $\epsilon_t \simeq \epsilon_m$ and Eq. 22a simplifies to:

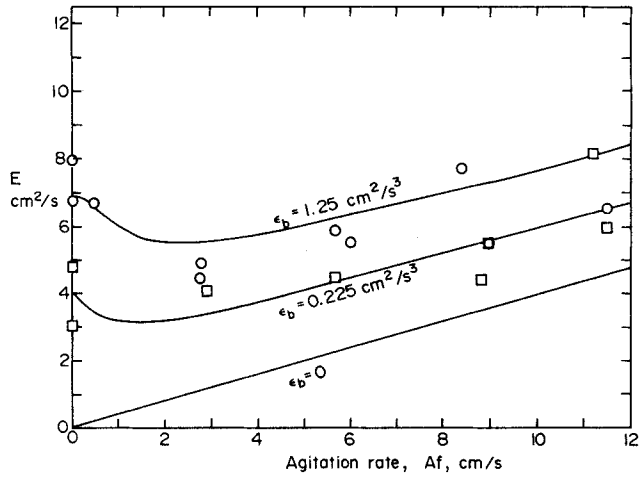

Figure 9. Effect of agitation on axial dispersion coefficient with buoyant energy dissipation as a parameter.

Lines represent Eq. 18 with values of ϵ_b as indicated (cm²/s³). $h = 5.2$ cm

Data point symbol:	O	□
Range of ϵ_b (cm²/s³):	1.0 to 1.5	0.2 to 0.25

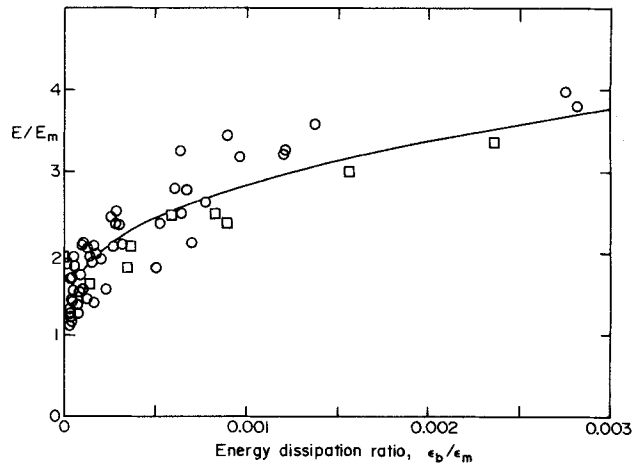

Figure 10. Enhancement of axial dispersion by buoyant energy dissipation.

Line represents Eq. 22b with ℓ_m = 0.301 cm, ℓ_b = 4.02 cm
O hot/cold water □ salt solution

$$E/E_m = [1 + ((\ell_b/\ell_m) - 1)(\epsilon_b/\epsilon_m)^{.34}]^{4/3} \qquad (22b)$$

In this work, E_m is given by Eq. 21 and the ratio of mixing lengths (ℓ_b/ℓ_m) is 13.3. Thus, Eq. 22b provides a simple relation between the enhancement of axial mixing and the ratio of energy dissipation rates, ϵ_b/ϵ_m. This function is compared with experimental data in Figure 10 for energy ratios up to 0.003. Despite the extremely small ratios of buoyant energy dissipation to mechanical energy dissipation, the enhancements are significant. The nonlinear nature of Eq. 22b indicates a steep initial increase of E as soon as ϵ_b exceeds zero. This shows that in measuring E, extreme care is needed to ensure that any tracer solutions used should be neutrally buoyant.

Conclusions and Recommendations

The steady-state measurements with hot and cold water and with salt solutions have confirmed the earlier conclusions of Holmes et al. (1991) that axial dispersion in reciprocating plate columns is increased significantly by unstable density gradients. This work has focused on the effects of very small density gradients, and the results suggest a dependence of the effective mixing length on the energy dissipation rates due to buoyancy and mechanical agitation, as given by Eq. 18. In the absence of mechanical agitation, the mixing length is large (about 70% of the column diameter), but it decreases rapidly as mechanical agitation is increased; therefore, the axial dispersion coefficients go through a minimum (Figure 9). Under given conditions of mechanical agitation, the presence of even a very small density gradient can significantly increase axial dispersion. Figure 10 indicates that E can be doubled when the buoyant energy dissipation is only 0.0002 of the mechanical energy dissipation.

In extraction columns where axial concentration gradients in the continuous phase lead to unstable density gradients (density increasing with height), increased axial mixing could reduce the performance considerably. The effects of buoyancy are not restricted to reciprocating plate extraction columns; other types of open-structure extraction columns should therefore also be studied.

Acknowledgment

The authors are grateful to the Natural Sciences and Engineering Research Council of Canada for financial support and to Dr. T. L. Holmes of the Otto H. York Company for useful discussions.

Notation

A = agitation stroke, cm
c = concentration, g/mL
C_o = orifice coefficient for perforated plates (taken as 0.6 in this work)
E = axial dispersion coefficient, $cm^2 \cdot s^{-1}$
E_o = axial dispersion coefficient in absence of agitation, $cm^2 \cdot s^{-1}$
E_m = axial dispersion coefficient in absence of buoyancy effects, $cm^2 \cdot s^{-1}$
f = agitation frequency, rpm or Hz
g = acceleration due to gravity, $cm \cdot s^{-2}$
h = plate spacing, cm
ℓ = mixing length, cm
ℓ_b = mixing length due to buoyancy, cm
ℓ_m = mixing length due to mechanical agitation, cm
n = exponent in Eq. 17
S = plate fractional open area
T = temperature, °C
T_1 = temperature at top of column, °C
T_2 = temperature of water at base of column, °C
U = superficial velocity, $cm \cdot s^{-1}$
x = temperature difference ratio as defined in Eq. 6
z = vertical distance (upward direction), cm

Greek letters

ϵ_b = buoyant energy dissipation rate, W/kg or $cm^2 \cdot s^{-3}$
ϵ_m = mechanical energy dissipation rate, W/kg or $cm^2 \cdot s^{-3}$
ϵ_t = total energy dissipation rate, W/kg or $cm^2 \cdot s^{-3}$
$\Delta\rho$ = difference in density between continuous phase and pure water, g/mL
$\Delta\rho_{eff}$ = effective density difference (Eq. 14), g/mL
ρ = liquid density, g/mL

Literature Cited

Baird, M. H. I., and N. V. Rama Rao, "Characteristics of a Countercurrent Reciprocating Plate Bubble Column: II. Axial Mixing and Mass Transfer," *Can. J. Chem. Eng.*, **66**, 222 (1988).

Baird, M. H. I., and R. G. Rice, "Axial Dispersion in Large Unbaffled Columns," *Chem. Eng. J.*, **9**, 171 (1975).

Hafez, M. M., and M. H. I. Baird, "Power Consumption in a Reciprocating Plate Column," *Trans. Instn. Chem. Engrs.*, London, **56**, 229 (1978).

Hafez, M. M., M. H. I. Baird, and I. Nirdosh, "Flooding and Axial Dispersion in Reciprocating Plate Extraction Columns," *Can. J. Chem. Eng.*, **57**, 150 (1979).

Holmes, T. L., A. E. Karr, and M. H. I. Baird, "Effect of Unfavourable Continuous Phase Density Gradient on Axial Mixing," *AIChE J.*, **37**, 360 (1991).

Karr, A. E., "Performance of a Reciprocating Plate Extraction Column," *AIChE J.*, **5**, 446 (1959).

Kim, S. D., and M. H. I. Baird, "Axial Dispersion in a Reciprocating Plate Extraction Column," *Can. J. Chem. Eng.*, **54**, 81 (1976).

Perry, R. H., D. W. Green, and J. O. Maloney, eds., *Perry's Chemical Engineer's Handbook*, p. 3-75, 6th ed., McGraw-Hill, New York (1984).

Pratt, H. R. C., and M. H. I. Baird, "Axial Dispersion," Ch. 6, *Handbook of Solvent Extraction*, T. C. Lo, M. H. I. Baird, and C. Hanson, eds., Wiley-Interscience, New York (1983).

Rosen, A. M., and V. S. Krylov, "Theory of Scaling up and Hydrodynamic Modelling of Industrial Mass Transfer Equipment," *Chem. Eng. J.*, **7**, 85 (1974).

Manuscript received Mar. 12, 1991, and revision received June 3, 1991.